NASA CONTRACTOR REPORT

NASA CR-2096

NASA CR-20
c. 1

HIGHLY LOADED MULTI-STAGE
FAN DRIVE TURBINE -
LEANED STATOR CONFIGURATION DESIGN

by D. C. Evans and G. W. Wolfmeyer

Prepared by
GENERAL ELECTRIC COMPANY
Cincinnati, Ohio 45215
for Lewis Research Center

NATIONAL AERONAUTICS AND SPACE ADMINISTRATION • WASHINGTON, D. C. • JULY 1972

1. Report No. NASA CR-2096	2. Government Accession No.	3. Recipient's Catalog No.
4. Title and Subtitle HIGHLY LOADED MULTI-STAGE FAN DRIVE TURBINE - LEANED STATOR CONFIGURATION DESIGN		5. Report Date July 1972
		6. Performing Organization Code
7. Author(s) D. C. Evans and G. W. Wolfmeyer		8. Performing Organization Report No. GE R71 AEG 309
		10. Work Unit No.
9. Performing Organization Name and Address General Electric Company Cincinnati, Ohio 45215		11. Contract or Grant No. NAS 3-14304
		13. Type of Report and Period Covered Contractor Report
12. Sponsoring Agency Name and Address National Aeronautics and Space Administration Washington, D.C. 20546		14. Sponsoring Agency Code

15. Supplementary Notes

Project Manager, Thomas P. Moffitt, Fluid System Components Division, NASA Lewis Research Center, Cleveland, Ohio

16. Abstract

The results of the high lift blade configuration design study are reported. The three-stage constant-inside-diameter turbine utilizes a ten degree tangentially leaned stator in stage three. All other bladerows use plain blades. Analysis of the leaned stator is discussed, and detailed design data are summarized. Steady-state stresses are discussed, and the results of the mechanical design analysis are presented.

17. Key Words (Suggested by Author(s)) Turbine, High lift, Leaned stator turbine, Fan drive turbine, High stage loading	18. Distribution Statement Unclassified - unlimited		
19. Security Classif. (of this report) Unclassified	20. Security Classif. (of this page) Unclassified	21. No. of Pages 36	22. Price* $3.00

TABLE OF CONTENTS

LIST OF TABLES

LIST OF ILLUSTRATIONS

LIST OF SYMBOLS

A	Area ($in.^2$)
Aw	Axial width (in.)
C	Absolute velocity, $C = U+W$ (ft/sec)
c_p	Specific heat at constant pressure (ft^2/sec^2 °R)
C_f	Flow coefficient
D	Diameter (in.)
d_o	Throat dimension (in.)
F	Force (lbf)
Δh	Turbine energy extraction (Btu/lbm)
K_{bk}	Weight-flow blockage factor
1	Axial chord length along a streamline (in.)
M	Mach number
N	Rotational speed (rev/min)
n	Number of vanes or blades
P_S	Static pressure (psia)
P_T	Total pressure (psia)
R	Gas constant (ft^2/sec^2 °R)
r	Radial coordinate; radius (in.)
r_m	Radius of curvature of meridional pathline (in.)
T_{HLE}	Blade temperature at hub leading edge (°F)
T_S	Static temperature (°R)
T_T	Total temperature (°R)
t	Spacing (in.)
t_e	Trailing edge thickness (in.)

LIST OF SYMBOLS (Concluded)

σ_{Midcv} Stress at maximum distance from axis of least moment of inertia, concave surface (ksi)

σ_{lmi} Stress due to bending moment about axis of least moment of inertia (ksi)

σ_{mmi} Stress due to bending moment about axis of maximum moment of inertia (ksi)

ϕ Meridional angle; $\tan \phi = W_r/W_z$

ψ_{Zwei} Zweifel number

$\overline{\omega}_z$ Loss rate coefficient

Subscripts

h   Hub

i   Current axial station

i-1   Axial station immediately upstream of current station

m   Meridional component

p   Pitch

R   Relative

r   Radial component

t   Tip

u   Circumferential component

z   axial component

Operators

d   General differential change

D   Differential change following a particle

∂   Gradient in indicated direction

I. SUMMARY

The results of the detailed design of the high-lift blade configuration turbine for Task III of NASA Contract NAS3-14304 are presented. The high-lift device selected for use in the three-stage constant-inside-diameter turbine is a ten degree tangentially leaned stage three vane. All other bladerows use plain blading. The overall calculation scheme used in the analysis of the leaned vane turbine is described, and the radial-equilibrium equation used in the calculation is presented. Various degrees of vane tangential lean and axial sweep are investigated, and the final vane design is discussed. Detailed aerodynamic design data are summarized. Steady-state stresses are predicted and compared to the plain blade steady-state stresses. No stress problems are expected during air turbine testing.

II. INTRODUCTION

The development of high-bypass-ratio turbofan engines for future air-craft propulsion schemes requires the development of fan drive turbines with increasingly higher work output. The requirements of minimized weight and size of such turbofan engines produced a need for turbines with increasingly high stage loading. In order to maintain high turbine efficiencies at high stage loading, advances are required in the technology of producing increased aerodynamic load capability in turbine blading by means of improved design techniques and high-lift devices.

The specific objectives of this program are to:

- Investigate analytically and experimentally aerodynamic means for increasing the turbine stage loading and turbine blade load-ing consistent with high efficiency for multistage high loaded fan drive turbine configurations.

- Develop sufficient design information to determine the relative importance of changes in engine size, weight, and performance and give primary consideration to use of tandem rotors and stators, where applicable, to reduce weight or extend or improve the blading performance.

- Modify an existing three-stage highly loaded turbine rig and adapt the rig to an overall performance test program of sufficient extent so as to obtain blade element performance.

This is a 24-month analytical and experimental investigation program to provide a turbine high-stage-loading and high-blade-loading aerodynamic technology that will be specifically applicable to multistage fan drive turbine configurations for advanced high-bypass-ratio turbofan propulsion system application. The program will be divided into two phases encompassing nine task items of activity.

The first phase will cover Task Items I, II and III of the program which are to investigate requirements of selected advanced high-bypass-ratio turbo-fan systems, to carry out parametric turbine vector diagram studies, to con-duct a cascade test and evaluation program, to select one design for future study, to complete a detailed aerodynamic turbine design for an existing rig, to complete the detailed blading aerodynamic design for the rig, to perform detailed blading mechanical design for the rig, to perform the turbine rig mechanical design, and to prepare the turbine rig modification drawings required to utilize the existing three-stage highly-loaded-fan turbine rig. The second phase will cover Task Items IV through IX of this program to fabricate, procure, vibration bench test, fatigue endurance test, and inspect the turbine rig modifications; to instrument and calibrate the rig

vehicle; to conduct a test program and to report progress, analysis, and design, as well as test and performance results.

The Task I vector diagram study results have been reported (Reference 1). Based on the results of this study, a velocity diagram was chosen for three highly-loaded turbine configurations: (1) a turbine using plain blades, (2) a turbine using tandem blades and (3) another turbine using high-lift devices. The purpose of this report is to present the Task III detailed design of the turbine using high-lift devices.

III. PRELIMINARY DESIGN

A. REQUIREMENTS

The design requirements for the turbines to be studied were based on engine fan drive turbine requirements. An existing three-stage highly loaded fan drive turbine rotating rig was modified for the test and performance phase of this program. Scaling of the turbine to utilize the existing facility was discussed in Reference 2, and the full size and scaled turbine requirements are repeated here.

Parameter	Full Size	Scaled
Average Pitch Loading, $\dfrac{gJ\Delta h}{2\Sigma U_p^2}$	1.5	1.5
Equivalent Specific Work, E/θ_{cr}, (Btu/lbm)	33.0	33.0
Equivalent Rotative Speed, $N/\sqrt{\theta_{cr}}$, (rev/min)	2000	3169
Equivalent Weight Flow, $W\sqrt{\theta_{cr}}\ \varepsilon/\delta$, (lbm/sec)	70	28
Inlet Swirl Angle (degrees)	0	0
Exit Swirl Angle Without Guide Vanes (degrees)	≤ 5	≤ 5
Maximum Tip Diameter (inches)	45.0	28.4
Number of Stages	3	3
$W\sqrt{T_T}/P_T$ at inlet	108.4	43.16
$\Delta h/T_T$	.0635	.0635
$N/\sqrt{T_T}$	87.7	138.98

On the basis of these design requirements, a velocity diagram was chosen to be used in the design of all three turbines. The selection of this velocity diagram was discussed in Reference 1, and the final velocity diagram calculation results were presented in Reference 2. The turbine aerodynamic flowpath used in the design of all three turbines is presented in Figure 1.

B. CONCEPTS CONSIDERED

Several high-lift turbine concepts were considered during the preliminary design phase. The objective of using high-lift devices was to see an improvement in turbine performance. Among the devices considered were:

1) Aerodynamic jet flaps utilizing trailing edge or tangential blowing and/or suction,

2) Endwall treatment such as extraction of boundary layer air from an upstream stator hub or tip region and injection of this bleed air as a jet flap in a downstream stator,

3) Streamline spacer rings or flow splitters on the diffusing rotor,

4) Alternate tandem blade designs such as partial span tandem blading,

5) Use of stators with axial sweep or tangential lean.

Preliminary studies indicated that stators with axial sweep or tangential lean could be effectively used to improve the performance of this turbine. Because it was believed that this concept has more potential for use in an actual engine application, this concept was selected to be used in the design of the high-lift turbine.

C. ANALYSIS OF STATOR LEAN AND SWEEP

The analysis of the turbine using stators with tangential lean or axial sweep was performed with the aid of a digital computer program which describes the axisymmetric flow field in the region of turbo-machinery blading. The overall calculation scheme of the computer program is summarized here. The flow is considered at a number of axial stations, and the radial-equilibrium equation, energy equation, and continuity condition are employed at each of them to determine the distribution of flow properties from hub to tip. It is necessary, however, that these distributions obtained separately at each station be consistent from station to station, and that the radial acceleration which a fluid particle undergoes as it passes from station to station be accounted for in the radial-equilibrium equation. This is done by assuming that the shape of a meridional streamline is adequately represented by a spline constrained at each axial station consistent with the continuity condition, and at upstream and downstream boundary stations by a selected orientation and shape. The radial acceleration is expressed in terms of the meridional streamline slope and curvature.

An iterative method of solution is implied. Meridional streamline shapes are assumed based on results from the previous iteration, and flow distributions at each axial station are found. These imply new meridional streamline shapes, and this iterative calculation is allowed to continue until the changes in streamline shapes between two successive calculations are small enough to satisfy a predetermined tolerance.

A significant feature of the computer program is the inclusion of terms in the radial-equilibrium equation which represent the blade action by a distributed body force field and the blade thickness by distributed blockage. The equation, which appears in Reference 3, wherein physical interpretation of the individual terms is presented, is restated here:

$$\frac{1}{\rho}\frac{\partial P_s}{\partial r} = \left(\frac{1 - M_z^2}{1 - M_m^2}\right)\left(\frac{C_u^2}{r} - \frac{D^2 r}{Dz^2}\; C_z^2\right)$$

$$+ \frac{W_r C_z}{1 - M_m^2}\left[\frac{\partial(r\,\tan\phi)}{r\partial r} + \frac{1}{\lambda}\frac{D\lambda}{Dz}\right] - F_u\frac{M_r M_u}{1 - M_m^2} + F_r \qquad (1)$$

The heat addition term has been omitted since, in the absence of transients, the blade surface and the fluid adjacent to it are at the same temperature. As suggested in Reference 3, the computer program includes a term to represent the heating effect of internal fluid friction, which encompasses all loss sources including shock waves:

$$- \frac{W_r C_z}{1 - M_m^2}\left(1 - \frac{P_s}{P_{T_R}}\right)\frac{\bar\omega_z}{\ell} \qquad (2)$$

The loss-rate coefficient, $\bar\omega_z$, is defined in Reference 3.

The radial and tangential components of the blade force may be expressed in terms of the axial change in angular momentum by means of the following relationships:

$$F_u = \frac{C_z}{r}\frac{D(rC_u)}{Dz} \qquad (3)$$

and

$$F_r = F_u\,\tan\xi \qquad (4)$$

By using the fact that the second derivative of the meridional streamline shape can be related to the meridional streamline curvature, $1/r_m$, and trigonometry to relate velocity components, equation (1) may be rewritten as follows:

6

$$\frac{1}{\rho}\frac{\partial P_s}{\partial r} = \frac{1-M_z^2}{1-M_m^2}\left\{\frac{C_u^2}{r} + \frac{C_z^2\sec^3\phi}{r_m} + \frac{C_z^2\tan\phi}{1-M_z^2}\left[\frac{\partial\,(r\tan\phi)}{r\partial r}\right.\right.$$

$$\left.\left. - \left(1-\frac{P_s}{P_{T_R}}\right)\frac{\bar{\omega}_z}{\ell}\right]\right\}$$

$$+ \frac{1}{1-M_m^2}\left\{C_z^2\tan\phi\,\frac{1}{\lambda}\,\frac{D\lambda}{Dz} + \left[M_z^2\,(U-C_u)\tan\phi\right.\right.$$

$$\left.\left. + (1-M_m^2)\,C_z\tan\xi\right]\frac{1}{r}\,\frac{D(rC_u)}{Dz}\right\} \qquad (5)$$

The terms on the right-hand side of equation 5 have been grouped such that the first set of braces includes terms which are present anywhere in the flow field while the second set of braces includes terms which occur only when calculations inside the axial extent of a blade row are desired. By specification of the applicable input parameters, the intrabladerow calculation may be performed in order that the effects of stator lean and sweep may be determined.

At each axial station where the rotating bladerow is influential, the enthalpy of the fluid is related to the fluid swirl velocity by the energy equation which may be found in the following form in Chapter VIII of Reference 4:

$$(U\,C_u)_i - (UC_u)_{i-1} = g\,J\,c_p\,(T_{T_i} - T_{T_{i-1}}) \qquad (6)$$

The static condition of the fluid is described by the use of the equation of state,

$$P_s = g\rho_s RT_s, \qquad (7)$$

and the specific heats are assumed to be constant. Application of the continuity condition in the form found in Chapter VIII of Reference 4,

$$W = 2\pi g \int_{r_h}^{r_t} K_{bk}\,\rho\,C_z\,rdr, \qquad (8)$$

in combination with the previous four equations yields a complete description of the flow at each axial station. With the flow field completely described, loading parameters and forces on the blading and walls are calculated from station data using geometric characteristics of the system where required.

IV. DETAILED DESIGN

A. TANGENTIAL LEAN

The velocity diagram calculation results presented in Reference 2 show an increase in static pressure across the stage three rotor hub, and a large static pressure gradient from hub to tip at the rotor inlet. Because of the presence of these conditions, efforts to improve turbine performance through the application of a high-lift device were concentrated on stage three. Analyses of the turbine were performed with the stage three stator vanes tangentially leaned ten degrees and fifteen degrees. Figure 2 compares the stage three pressure parameter for the ten and fifteen degree stator lean cases to the pressure parameter for the plain blade turbine design which used a stator with no lean. It is seen that a significant reduction was achieved in the static pressure rise across the rotor hub relative to the plain blade turbine design. The figure shows that with the ten degree tangentially leaned stator, the rotor hub becomes essentially an impulse section: the pressure parameter is nearly zero, indicating no diffusion from the rotor inlet station to the rotor exit station. Figure 3 shows a reduction in the static pressure gradient from hub to tip for the ten degree lean case. Therefore, the ten degree tangentially leaned stator was selected as the high-lift device.

The effects of the tangentially leaned stator are further illustrated in Figures 4 through 6. Figure 4 compares the stator exit station axial velocity as a function of radius for the various degrees of stator lean. Figure 5 compares the parameter ρC_z versus radius for the cases studied. Figure 6 shows the effects of the leaned stator on the ten percent flow stream tubes. The leaned stator causes the mass flow to shift radially inward as it passes through the rotor.

B. AXIAL SWEEP

Studies were conducted to determine whether a combination of tangential lean and axial sweep in the stage three stator would give a performance improvement. Figure 7 compares the ten degree tangentially leaned stator with no axial sweep to the ten degree tangentially leaned stator with forward axial sweep such that the stator leading edge is radial. Figure 8 shows that this combination of lean and sweep reduced the improvement in pressure parameter gained by the leaned stator with no sweep. It was believed that the use of aft sweep (stator hub trailing edge shifted in the aft direction relative to the tip trailing edge) would show some improvement, but only at the expense of increasing the already large axial gap between the stage two rotor hub trailing edge and the stage three stator hub leading edge. Further examination of stator axial sweep was not pursued.

8

C. BLADING AERODYNAMIC DESIGN

As a result of the studies discussed above, the stage three ten degree tangentially leaned stator was selected to be used in the high-lift turbine. The use of the leaned stator had a slight influence on the stage three blade inlet angles as shown in Figure 9. It was decided that this influence was not of enough significance to require a new stage three blade design as evidenced by the velocity distribution comparisons in Figures 10 through 12. Thus, all blading for the high-lift turbine remained the same as the plain blade turbine hardware with the exception of the stage three stator.

The stage three leaned stator uses the same number of vanes as the stage three plain blade stator. The vanes were leaned in such a manner that the stator total throat area was not changed from that of the plain blade stator. The vane section profiles which had been generated for the plain blade turbine were maintained. The sections were stacked on the trailing edge; however, because the tangentially leaned stator trailing edge is longer than that of the plain stator, new vane section locations were required, and the new locations are specified in Figure 13. The vane sections are shown in a reduced copy of the precision master (Figure 14) used in the vane fabrication.

Table I summarizes the ten degree tangentially leaned stage three vane design data. Nomenclature used in the summary is defined in Figure 15.

V. MECHANICAL DESIGN

A. VIBRATORY BEHAVIOR

Because none of the rotor blading was changed from that of the plain blade turbine, a new vibratory behavior analysis was not required. The predicted vibratory behavior of the blades may be found in Reference 2.

B. STEADY-STATE BEHAVIOR

Because the ten degree tangentially leaned vane changed the static pressure gradient ahead of the stage three blade, new spanwise blade loading distributions resulted. Figure 16 compares the new blade loadings to the plain blade loading. Steady-state mechanical stresses were calculated on the basis of the new blade loadings for the free slip tip shroud boundary condition (blade fixed at the base of the shank, adjacent tip shrouds allowed to slip relative to each other), which was believed to be the most realistic for steady-state operation. The results of the analysis, as summarized in Table II, show that all of the important steady-state stress and vibratory capability parameters remain virtually unchanged from those of the plain blade turbine. The blade remains quite acceptable, and no stress problems are expected during air turbine testing.

C. KEY DETAIL DRAWINGS

The mechanical design flowpath for the air turbine test rig is shown in Figure 17. The key detail drawings used in the assembly of the tangentially leaned stage three vane are:

Drawing 4013098-613   Turbine, Vane -- High-Lift
                            Stage 3 NASA HLMSFT

Precision Master 4012241-991   High-Lift Vane 3
                            NASA HLMSFT

Other key detail drawings used in the turbine assembly were summarized in Reference 2.

REFERENCES

1. Evans, D.C.: "Investigation of a Highly Loaded Multistage Fan Drive Turbine, Report for Task I - Vector Diagram Study," NASA CR - 1862, July 1971.

2. Evans, D.C. and Wolfmeyer, G.W.: "Investigation of a Highly Loaded Multistage Fan Drive Turbine - Plain Blade Configuration Design," NASA CR-1964, November 1971.

3. Smith, L.H., Jr.: "The Radial-Equilibrium Equation of Turbomachinery," ASME Paper No. 65-WA/GTP-1, Journal of Engineering for Power, Trans. ASME, Series A, Vol. 88, 1966.

4. Lewis Research Center, NASA: "Aerodynamic Design of Axial Flow Compressors, Revised," NASA SP-36, 1965.

TABLE I. STAGE THREE TANGENTIALLY LEANED VANE DESIGN DATA

Parameter	Hub	Pitch	Tip
Diameter (trailing edge, in.)	17.80	22.61	27.42
α_o, (degrees)	46.13	39.60	38.00
α_1, (degrees)	56.99	52.20	51.65
ψ_{Zwei}, incompressible	0.860	0.879	0.852
Aw, (in.)	1.00	1.30	1.60
t, (in.)	0.559	0.710	0.861
n	100	100	100
nd_o (C_f = .975 η_V = .97)	30.700	43.800	53.700
$d_o = nd_o/n$ (in.)	0.307	0.438	0.537
t_e, (in.)	0.020	0.020	0.020
$t_e/(t_e + d_o)$	0.061	0.044	0.036
Chord, (in.)	1.062	1.374	1.681
$t_{max.}$, max thickness (in.)	0.090	0.109	0.128
Unguided turning (degrees)	8.80	8.10	6.40
Overturning (degrees)	0.70	1.00	2.80
Wedge angle (degrees)	5.50	5.30	5.00
Tangential lean, ξ, (degrees)	---	10.00	---

Precision Master No. 4012241-991

Table II. STEADY-STATE MECHANICAL STRESSES AND ESTIMATED VIBRATORY CAPABILITIES

Mechanical Stresses (ksi)			Stage Three Blade
Airfoil Hub			
σ centrifugal			9.41
σ maximum gas bending (LE)			14.76
σ resultant span wise	LE		24.12
stress (free slip mode)	TE		19.01
	Hi-c		2.21
	Midcv		8.03
σ uncorrected gas bending	LE		14.32
(lmi and mmi, free	TE		14.91
slip mode)	Hi-c		−8.41
	Midcv		−1.65
σ corrected gas bending	LE		11.74
(lmi and mmi,	TE		11.95
free slip mode)	Hi-c		−6.82
	Midcv		−1.34
Under Tip Shroud			
σ centrifugal			7.18
σ resultant span wise	LE		27.66
stress (free slip mode)	TE		22.73
	Hi-c		−0.89
	Midcv		2.13

Estimated Vibratory Capabilities

$$\sigma_{mean} = \sigma_c + \sigma_{lmi} + \sigma_{mmi} \text{ (ksi)}$$ 24.17

at Hub LE ($\sigma_{thermal}$ neglected)

Estimated T_{HLE} (°F)   113.00

Estimated Minimum Margin   36.20
Vibratory Allowable Stress
(ksisa) (Based on AISI 410 Stainless
steel average strength less three
standard deviations)
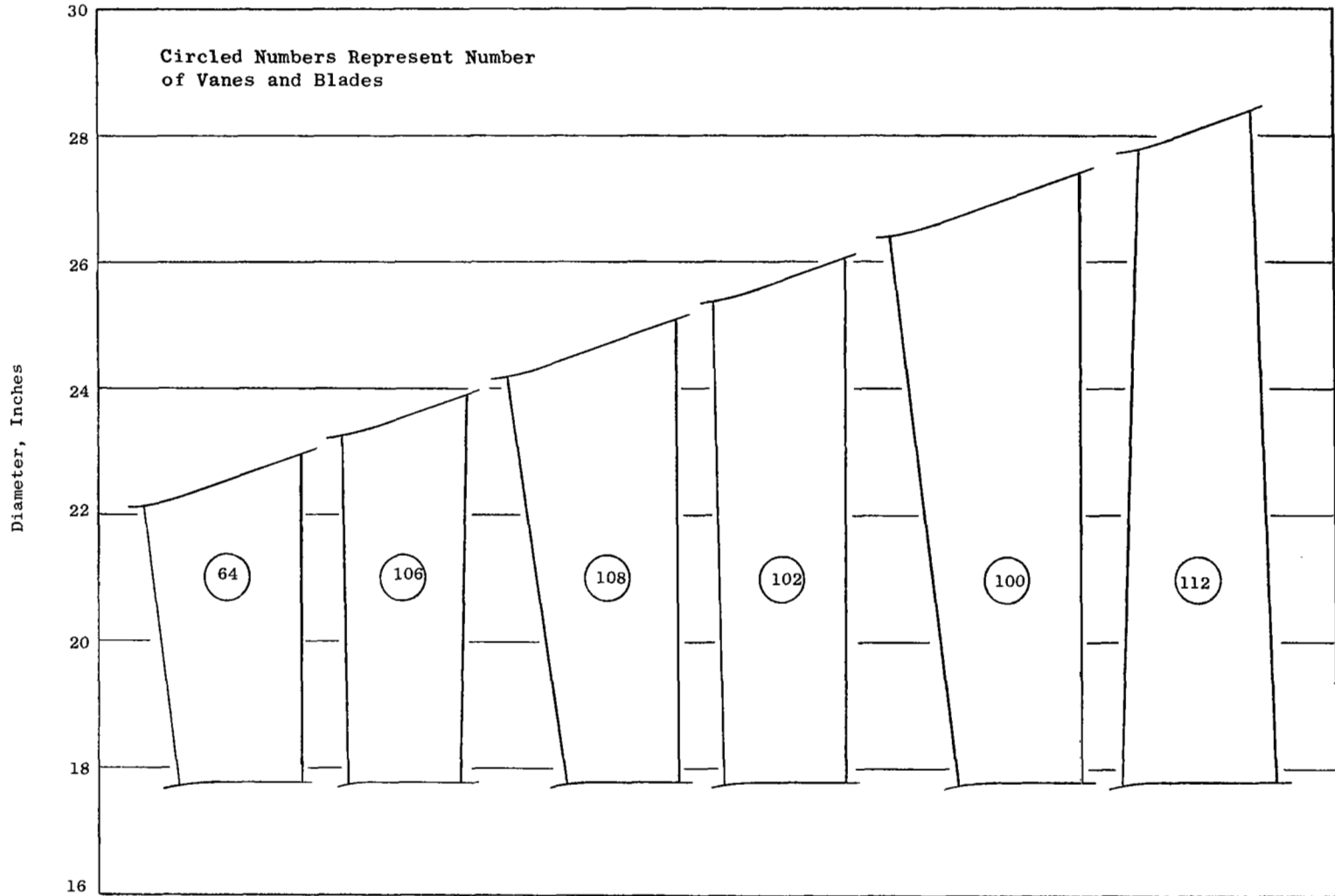
Figure 1.   Turbine Aerodynamic Flowpath.
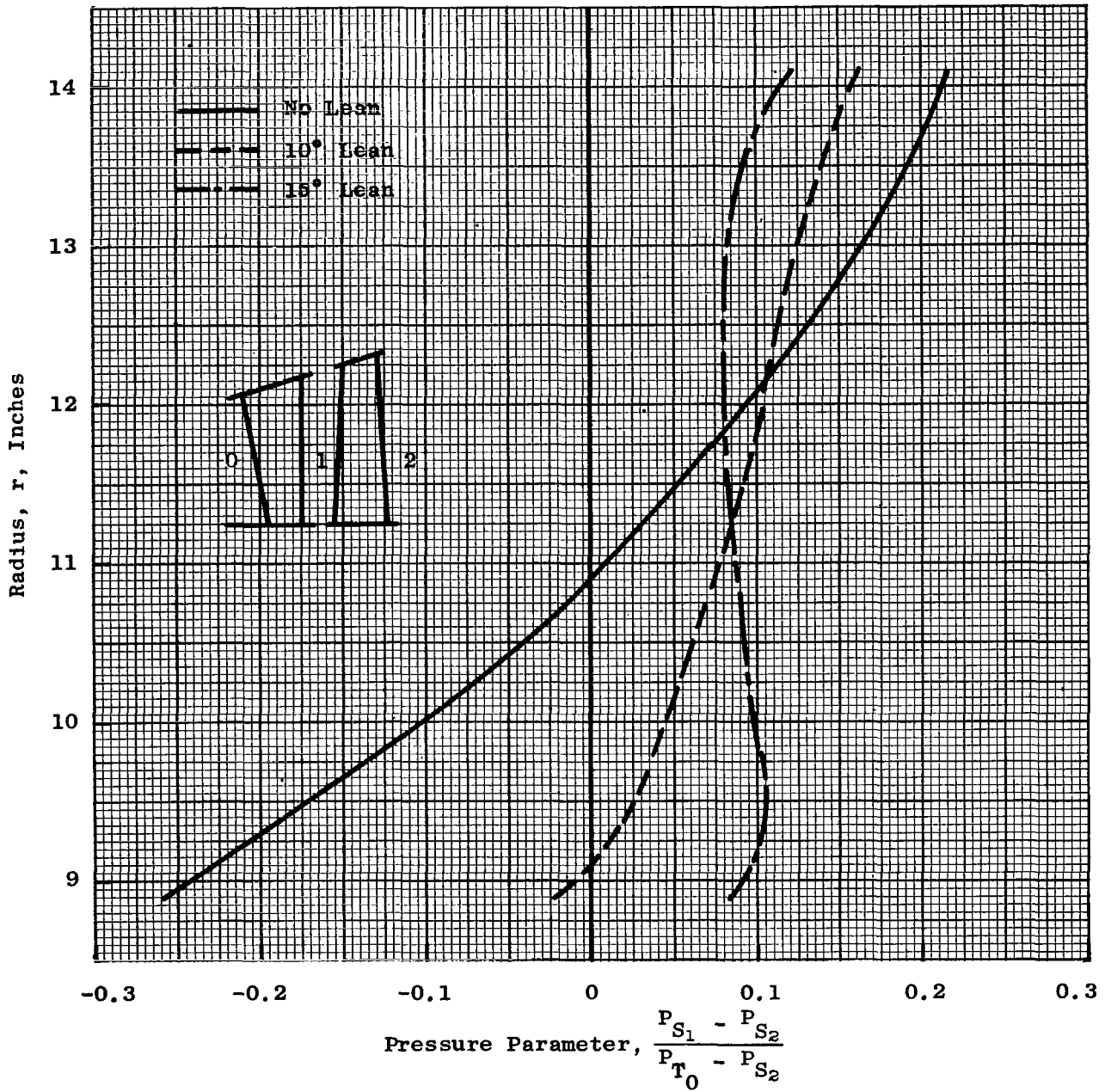
Figure 2. Effect of Stage Three Vane Lean on Pressure Parameter.
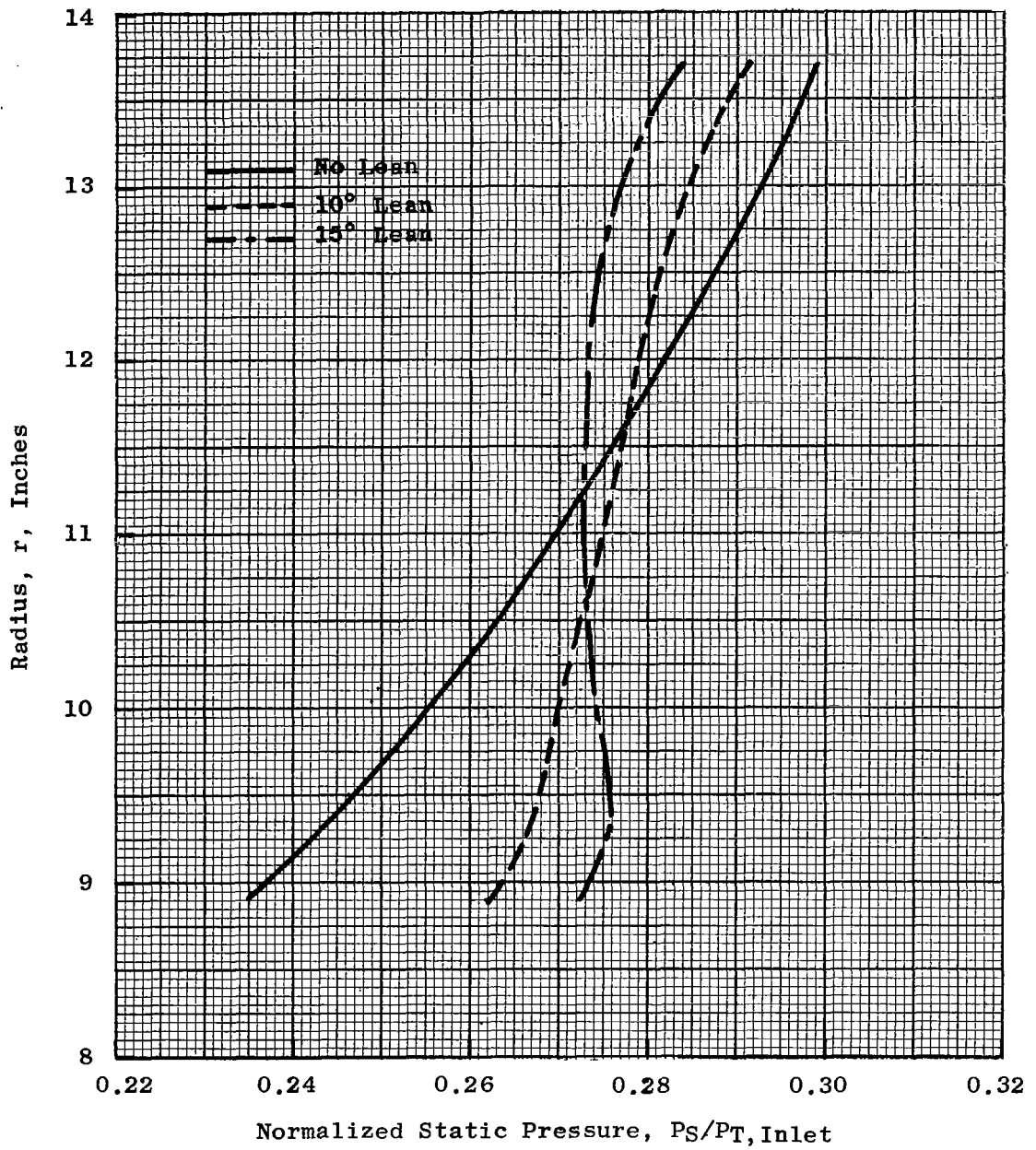
Figure 3. Effect of Stage Three Vane Lean on Static Pressure Gradient at Vane Exit.

16
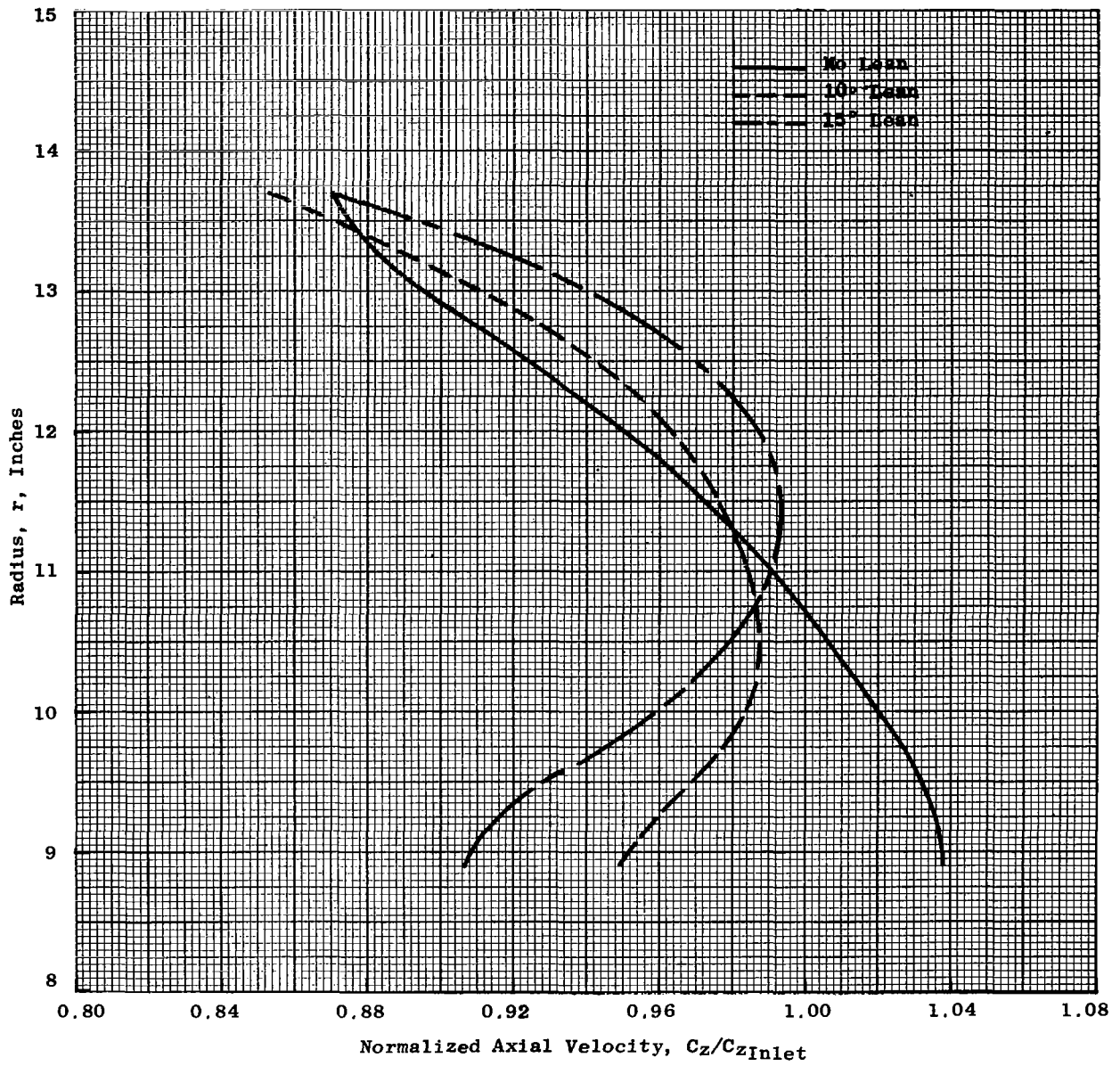
Figure 4. Effect of Stage Three Vane Lean on Axial Velocity at Vane Exit.
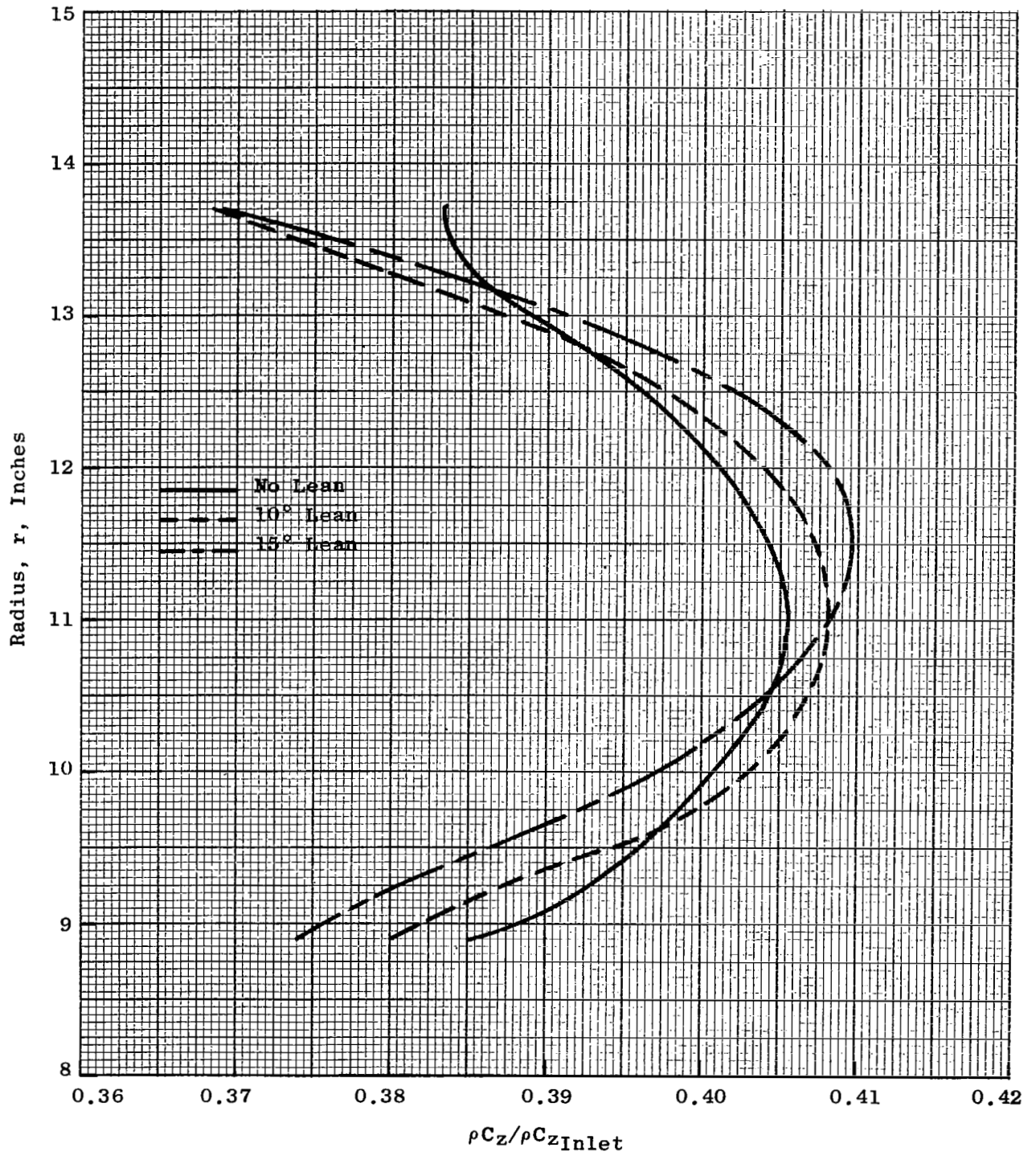
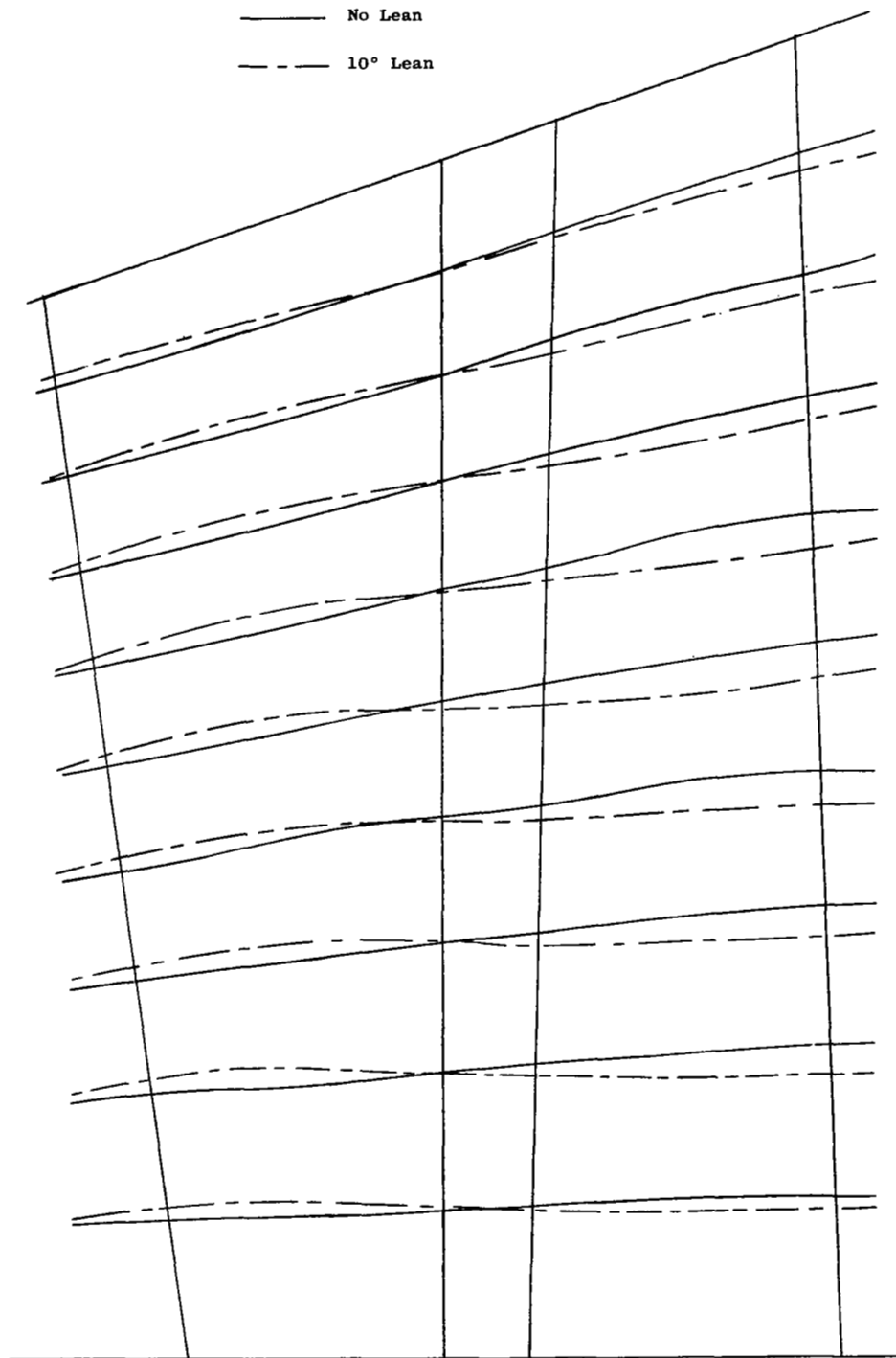Figure 5. Effect of Stage Three Vane Lean on ρC_z at Vane Exit.

Figure 6. Effect of Stage Three Vane Lean on
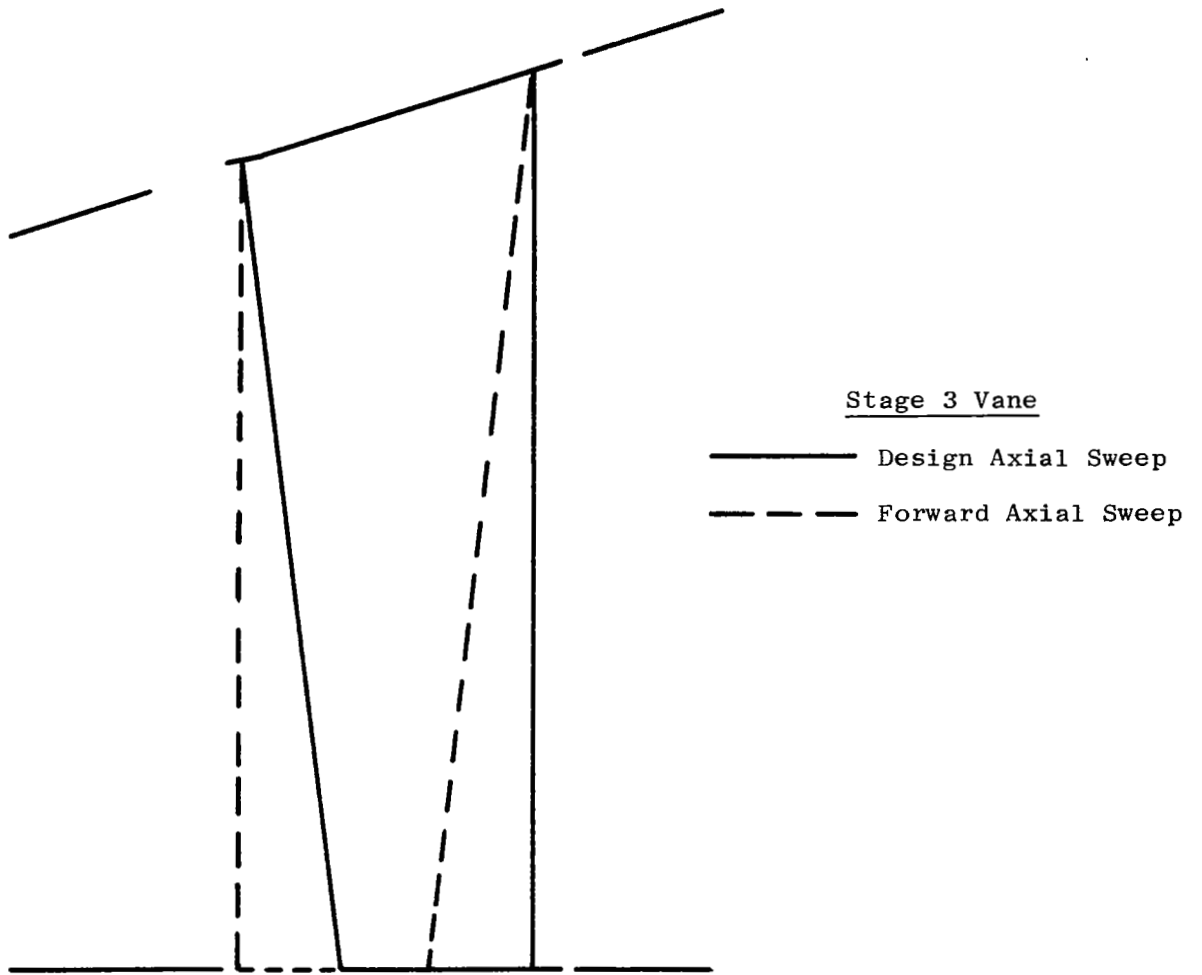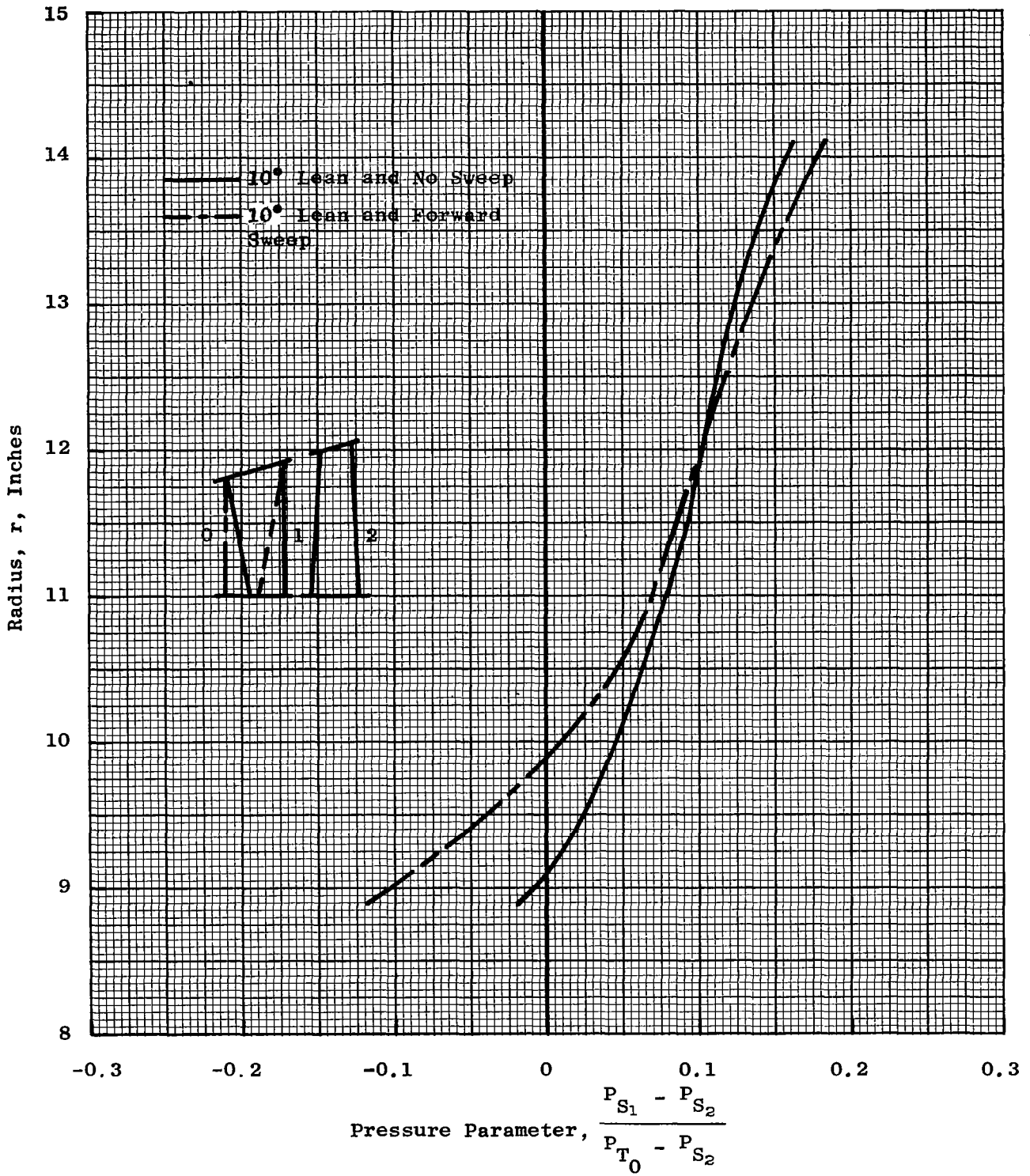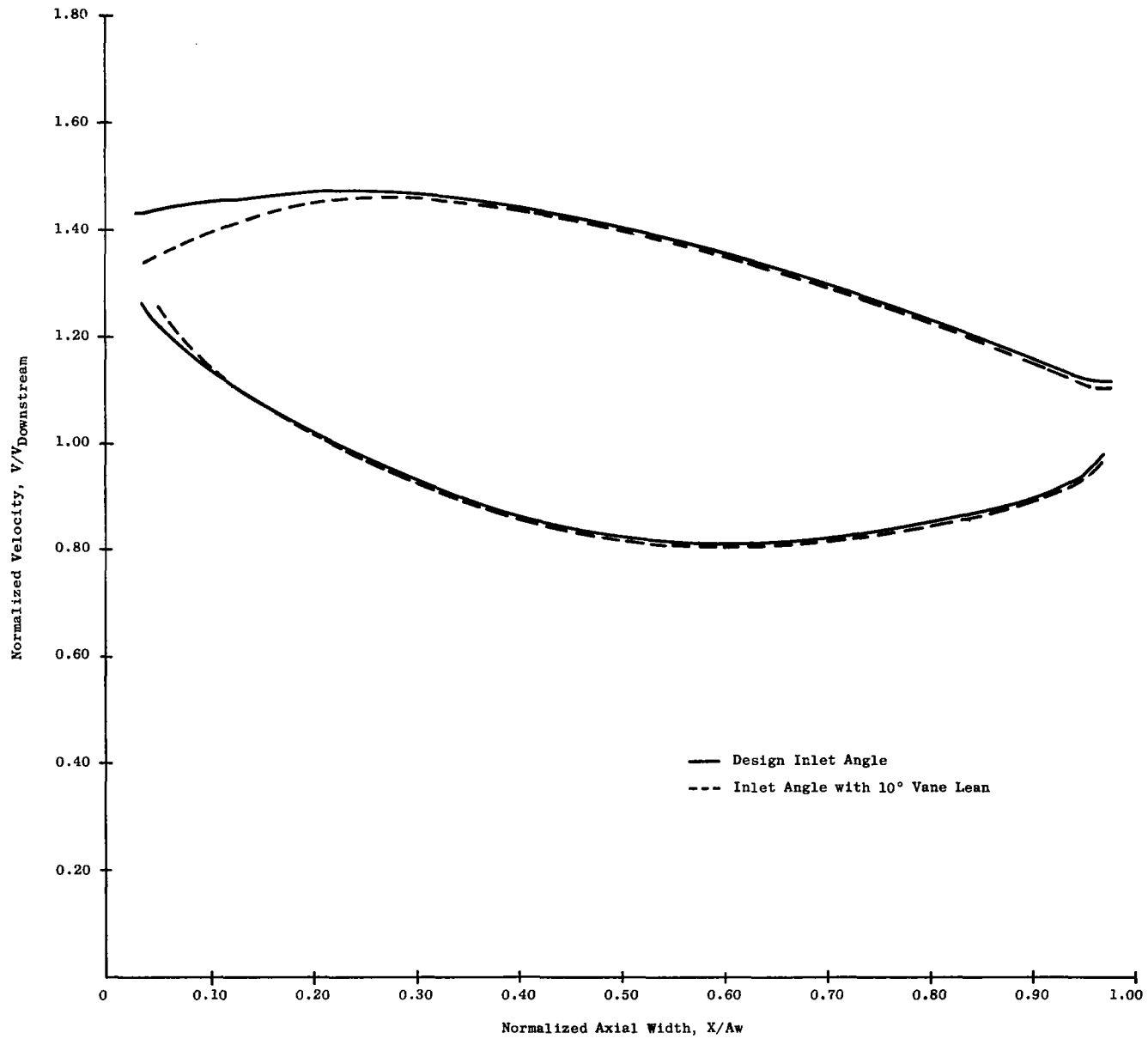Streamline Through Stage Three.

19

Stage 3 Vane

—————— Design Axial Sweep

— — — Forward Axial Sweep

Figure 7. Vane Axial Sweep.

Figure 8. Effect of Stage Three Vane Axial Sweep on Pressure Parameter.
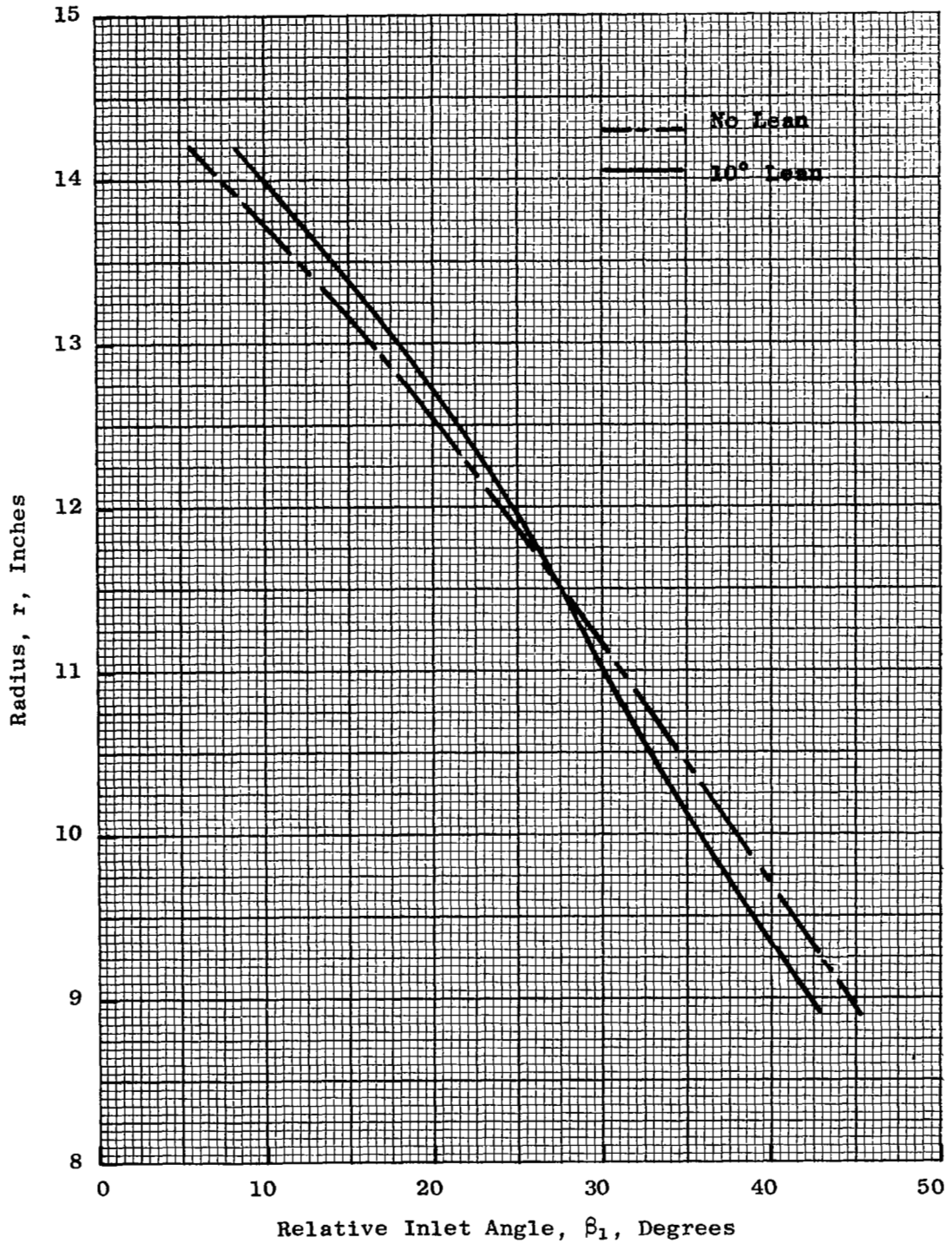
Figure 9. Effect of Stage Three Vane Lean on Stage Three Blade Inlet Angles.

Figure 10. Stage Three Blade Hub Velocity Distribution.

Note: No Change from Design Inlet Angle
       when Using 10° Leaned Vane.
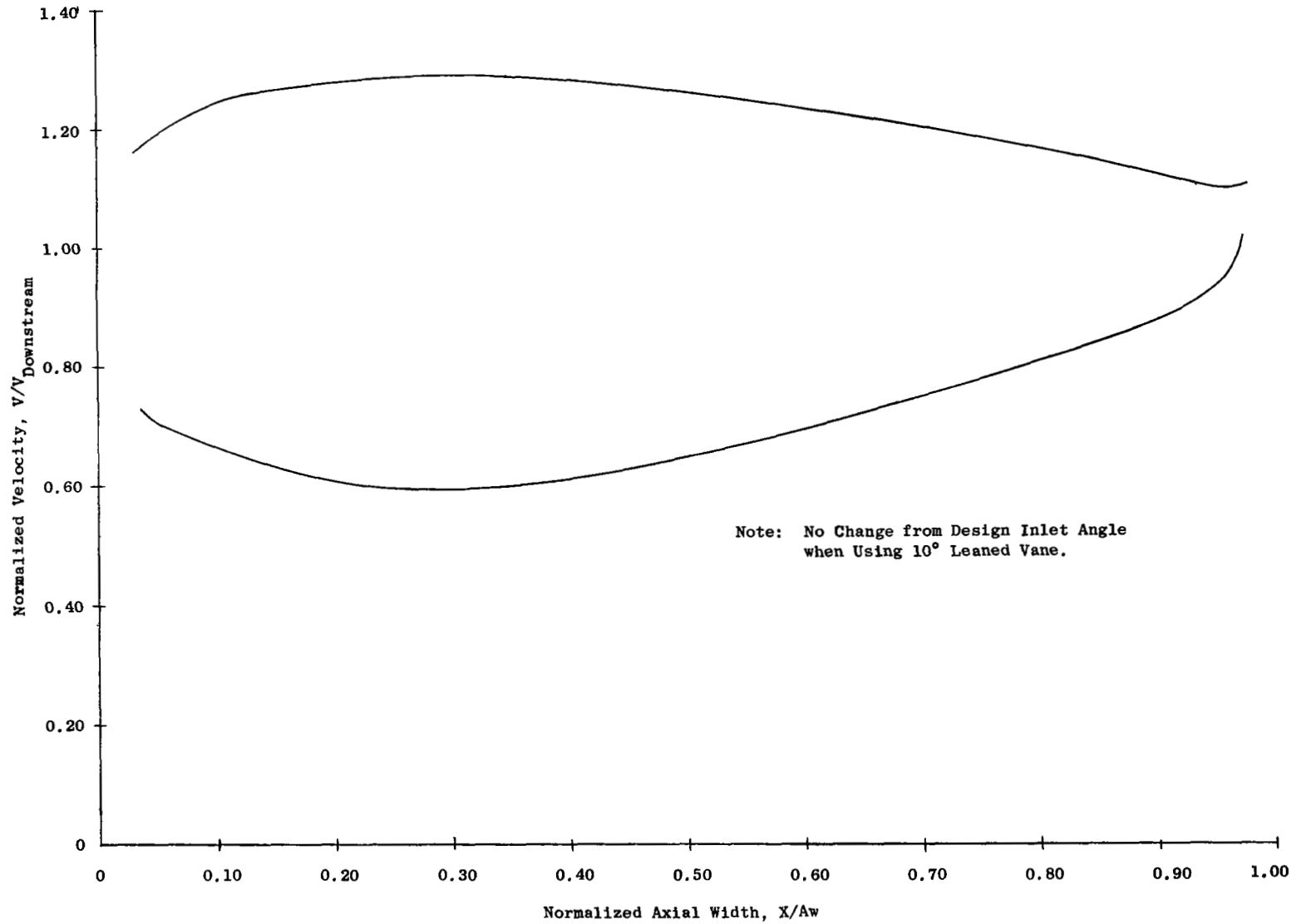
Figure 11. Stage Three Blade Pitch Velocity Distribution.
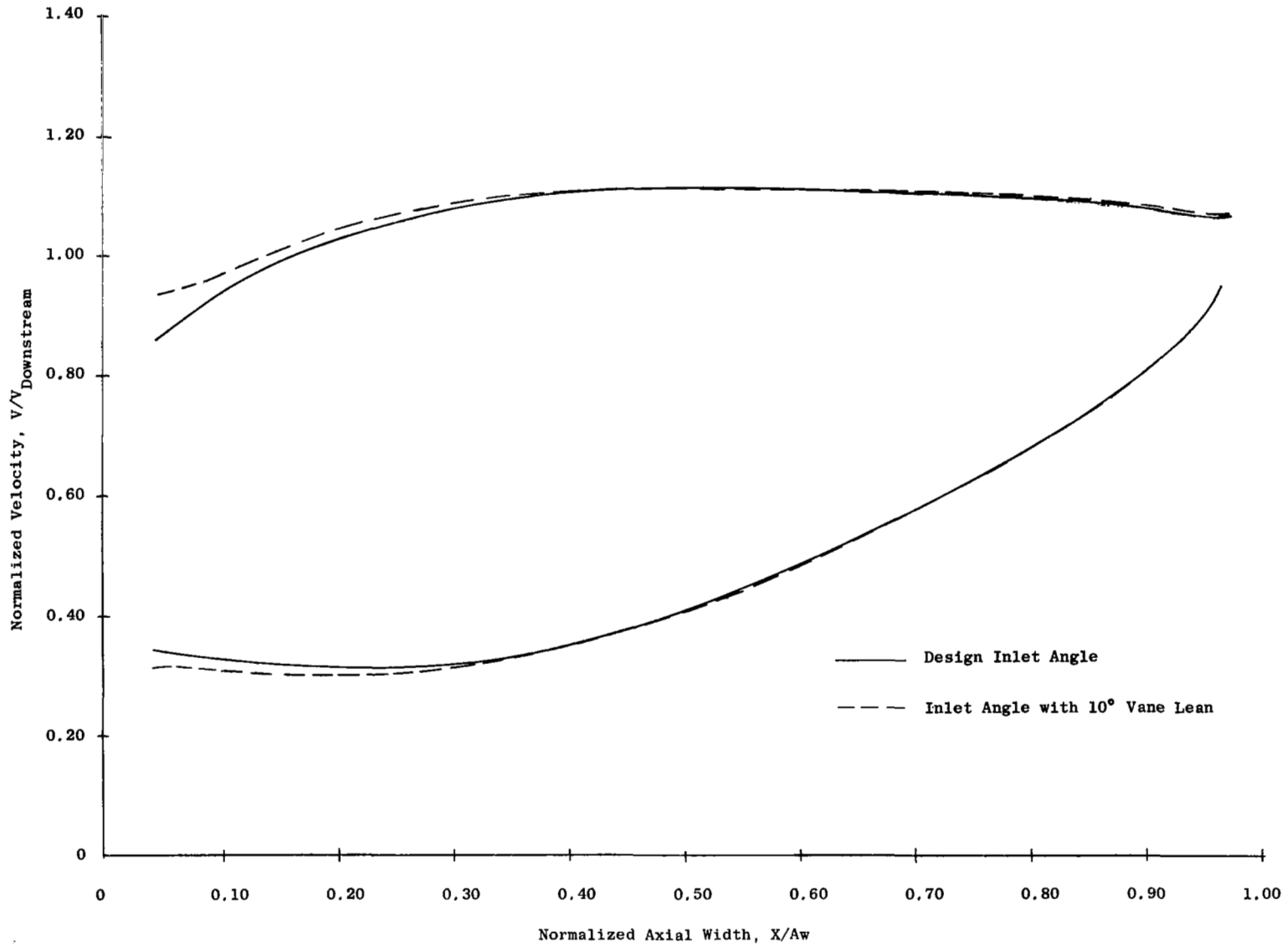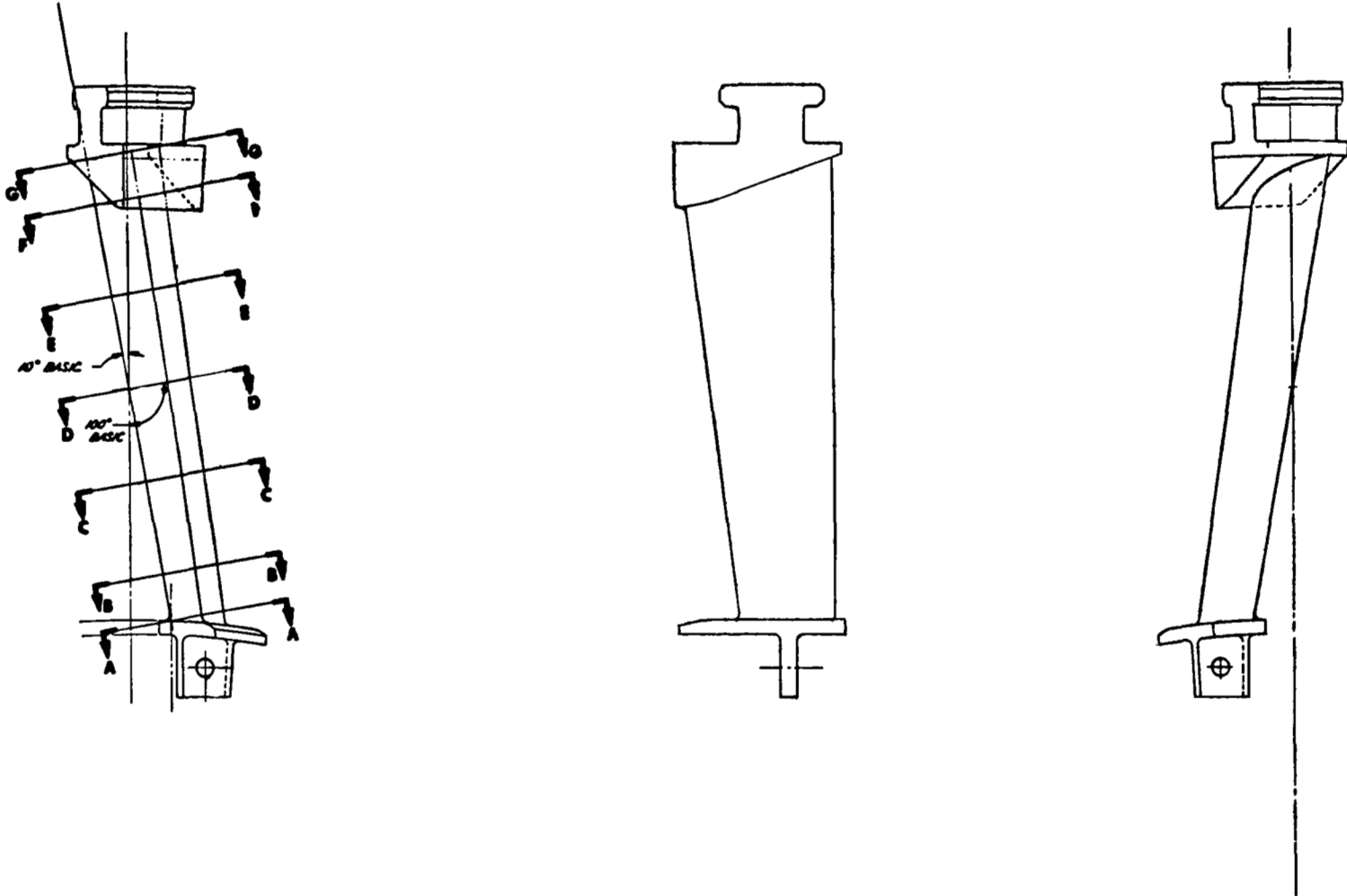
Figure 12. Stage Three Blade Tip Velocity Distribution.

The chart shows Normalized Velocity, V/V_Downstream (y-axis, from 0 to 1.40) versus Normalized Axial Width, X/Aw (x-axis, from 0 to 1.00). Legend: solid line — Design Inlet Angle; dashed line — Inlet Angle with 10° Vane Lean.

Figure 13. Stage Three 10-Degree Tangentially Leaned Vane.
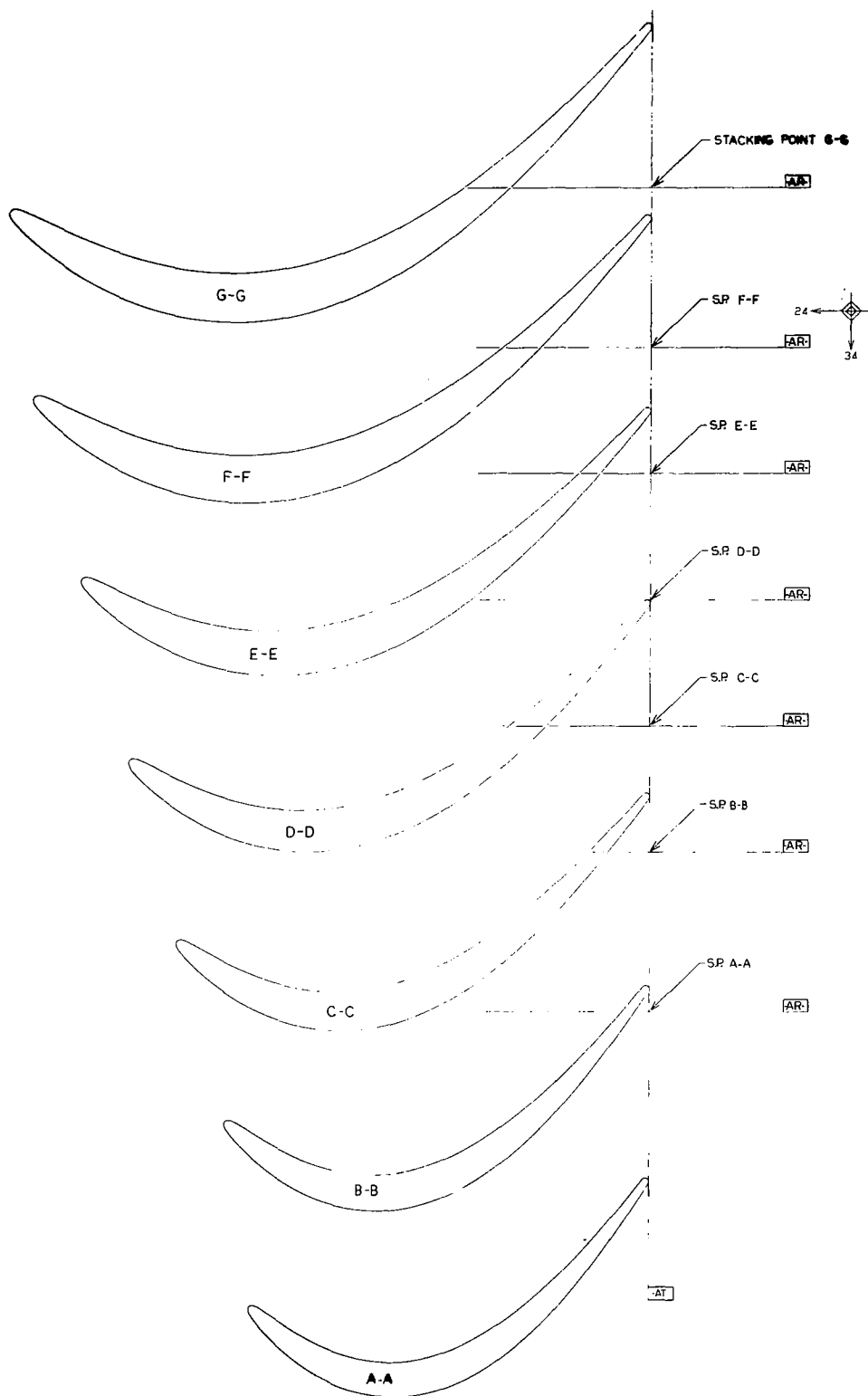
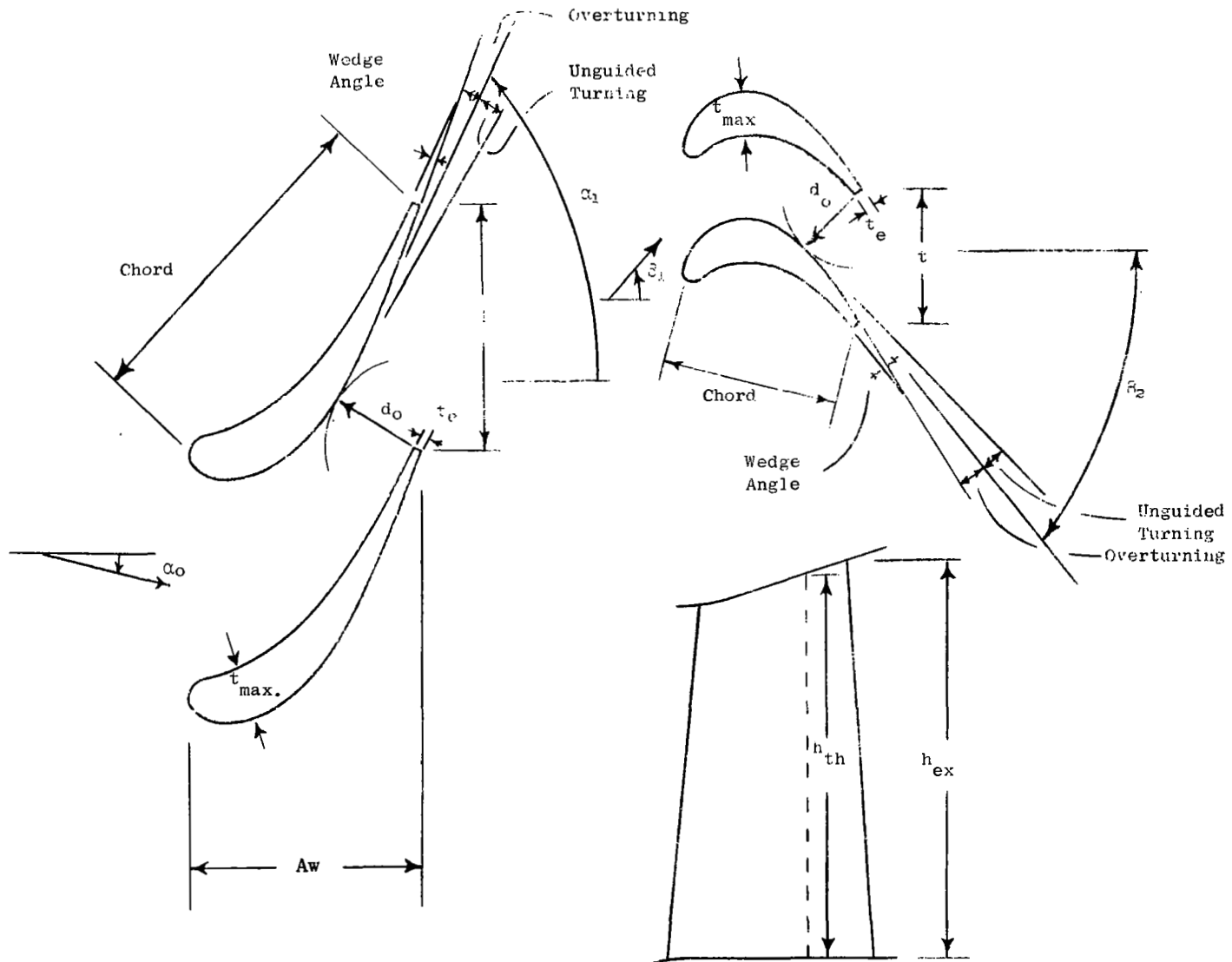Figure 14.   Stage Three Vane Precision Master
(4012241-991).

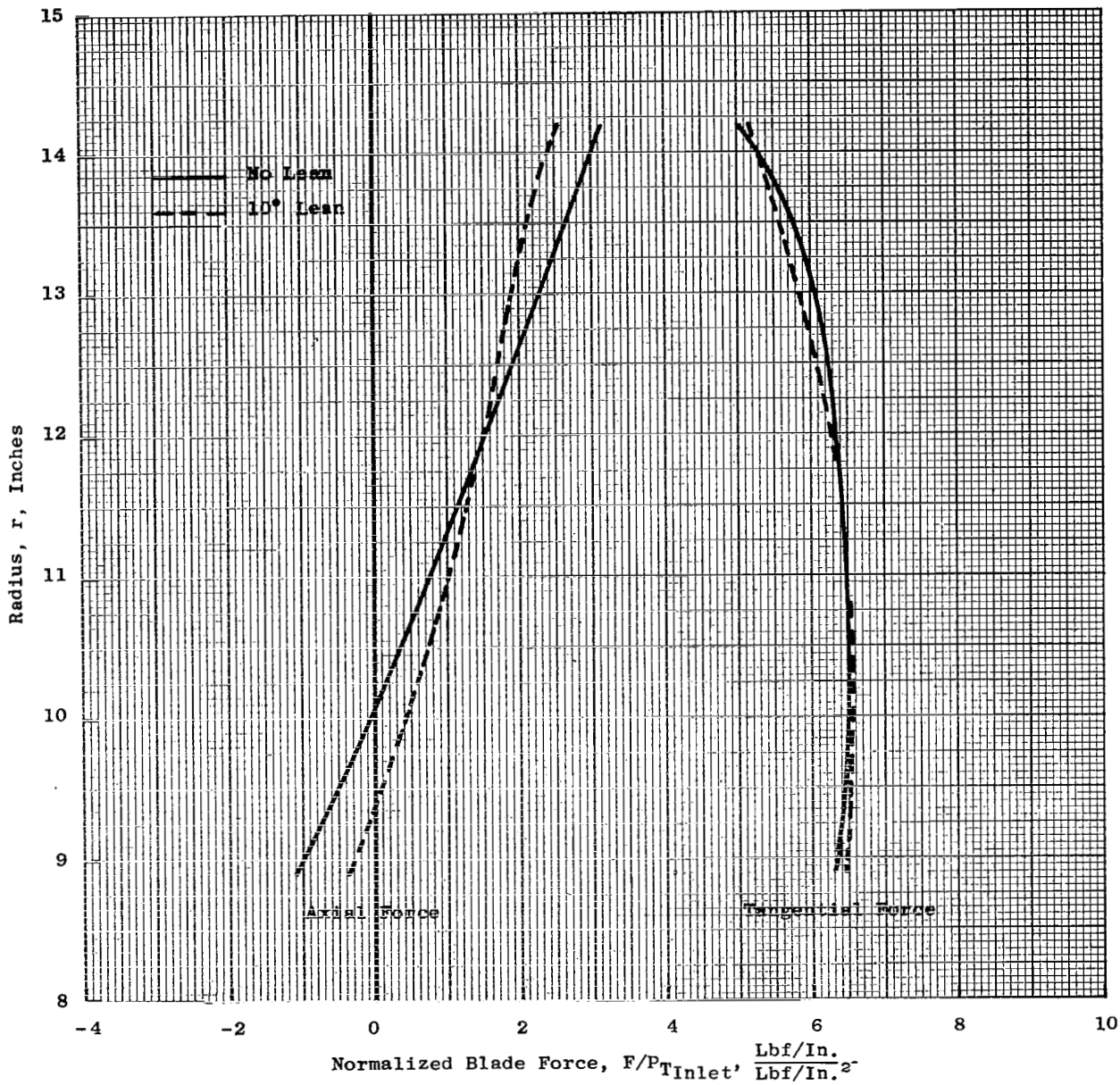Figure 15. Design Data Nomenclature.

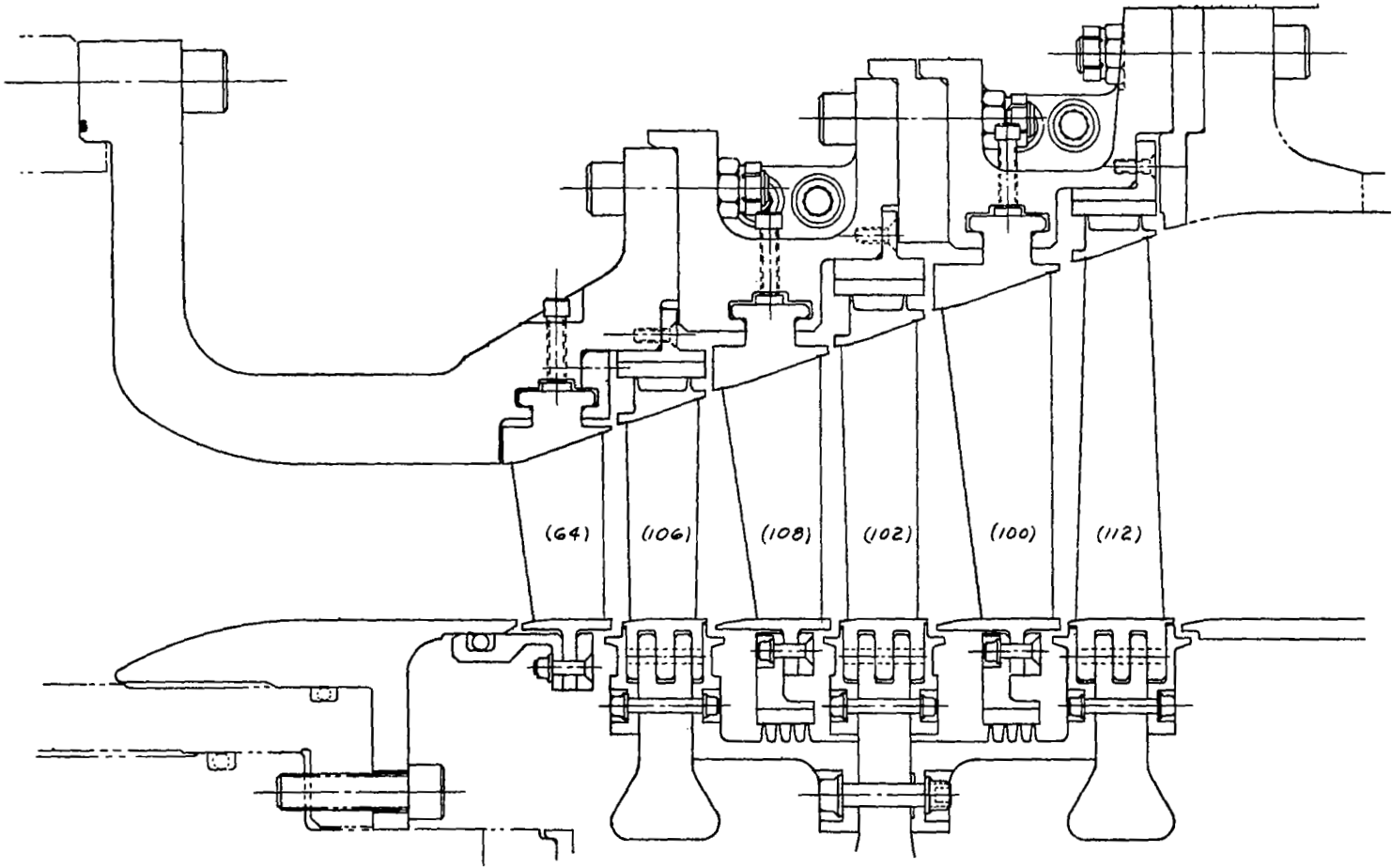Figure 16. Stage Three Blade Spanwise Loading Distribution.

(64) (106) (108) (102) (100) (112)

Figure 17. Mechanical Design Flowpath.